Control of cerebellar granule cell output by sensory-evoked Golgi cell inhibition

Ian Duguid[1,2,3], Tiago Branco[1,4], Paul Chadderton[5], Charlotte Arlt, Kate Powell[6], and Michael Häusser[3]

Wolfson Institute for Biomedical Research and Department of Neuroscience, Physiology, and Pharmacology, University College London, London WC1E 6BT, United Kingdom

Edited by Masao Ito, RIKEN Brain Science Institute, Wako, Japan, and approved September 1, 2015 (received for review May 25, 2015)

Classical feed-forward inhibition involves an excitation–inhibition sequence that enhances the temporal precision of neuronal responses by narrowing the window for synaptic integration. In the input layer of the cerebellum, feed-forward inhibition is thought to preserve the temporal fidelity of granule cell spikes during mossy fiber stimulation. Although this classical feed-forward inhibitory circuit has been demonstrated in vitro, the extent to which inhibition shapes granule cell sensory responses in vivo remains unresolved. Here we combined whole-cell patch-clamp recordings in vivo and dynamic clamp recordings in vitro to directly assess the impact of Golgi cell inhibition on sensory information transmission in the granule cell layer of the cerebellum. We show that the majority of granule cells in Crus II of the cerebrocerebellum receive sensory-evoked phasic and spillover inhibition prior to mossy fiber excitation. This preceding inhibition reduces granule cell excitability and sensory-evoked spike precision, but enhances sensory response reproducibility across the granule cell population. Our findings suggest that neighboring granule cells and Golgi cells can receive segregated and functionally distinct mossy fiber inputs, enabling Golgi cells to regulate the size and reproducibility of sensory responses.

cerebellum | Golgi cells | granule cells | inhibition | synaptic integration

Classical feed-forward inhibition (FFI) involves a sequence of excitation rapidly terminated by inhibition. This temporal sequence narrows the time window for synaptic integration and enforces precise spike timing (1–7). FFI is thought to be important for regulating the temporal fidelity of spike responses in many neural systems, including the motor system, where rapid and adaptable changes in muscle activity are essential for coordinated motor control (8–10). The cerebellum plays a central role in fine sculpting of movements, and damage to the cerebellum produces severe motor deficits, most notably enhanced temporal variability of voluntary movements (11, 12). These findings suggest that cerebellar circuits have the ability to preserve precise timing information during behavior (5, 6, 13), and in vitro studies have shown that feed-forward inhibitory networks in the input layer of the cerebellum provide a mechanism for maintaining the temporal fidelity of information transmission (6, 14, 15).

Synaptic inhibition in the granule cell layer is generated by Golgi cells, GABAergic interneurons that provide direct inhibitory input to granule cells (6, 15–17). The prevailing view is that, when mossy fibers are activated, granule cells receive both monosynaptic excitation and disynaptic FFI from Golgi cells, providing temporally precise inhibitory input that narrows the window for the temporal summation of discrete mossy fiber inputs (6, 14, 18). This classical excitation–inhibition sequence forms the basis of a variety of contemporary cerebellar models (7, 9, 18, 19). However, the exact temporal relationship between sensory-evoked excitation and inhibition in granule cells has never been determined in vivo. Here, we combined in vivo whole-cell voltage-clamp recordings from granule cells and in vitro dynamic clamp experiments to investigate both the temporal dynamics of Golgi-cell–mediated inhibition and its importance for shaping sensory responses in the input layer of the cerebellum.

Results

Sensory-Evoked Phasic and Spillover Golgi Cell Inhibition Precedes Mossy Fiber Excitation in Granule Cells. Cerebellar granule cells receive direct phasic and indirect or "spillover" GABAergic input from Golgi cells (6, 16, 20, 21). To investigate the temporal dynamics of sensory-evoked inhibition in vivo, we recorded spontaneous and sensory-evoked excitatory (V_{hold} = −70 mV) and inhibitory (V_{hold} = 0 mV) currents from the same granule cells in Crus II (Fig. 1 *A–D*). Granule cells were identified based on their characteristic electrophysiological properties (Table S1), depth from the pial surface (>250 μm), and morphology (Fig. 1*B*). To evoke behaviorally relevant somatosensory input, we applied brief air puffs (60 ms) to the whiskers and ipsilateral perioral surface (22, 23). Sensory stimulation triggered bursts of mossy fiber excitatory postsynaptic currents (EPSCs; 4.9 ± 0.6 events; burst frequency, 104.0 ± 10.3 Hz; burst duration, 54.8 ± 4.0 ms) (23–25). The same sensory stimulus also triggered phasic inhibitory postsynaptic currents (IPSCs; 5.6 ± 0.6 events; burst frequency, 65.5 ± 8.8 Hz; burst duration, 93.3 ± 15.1 ms) in the same granule cells (n = 9 of 9 cells) (Fig. 1 *C* and *D*). Each

Significance

Understanding how synaptic inhibition regulates sensory responses is a fundamental question in neuroscience. In cerebellar granule cells, sensory stimulation is thought to evoke an excitation–inhibition sequence driven by direct input from mossy fibers and followed by classical disynaptic feed-forward inhibition from nearby Golgi cells. We made, to our knowledge, the first voltage-clamp recordings of sensory-evoked inhibition in granule cells in vivo and show that, surprisingly, sensory-evoked inhibition often precedes mossy fiber excitation activated by the same stimulus. We demonstrate how such "preceding" inhibition can shape granule cell responses to sensory stimulation. Our findings challenge the existing view that classical feed-forward inhibition is the dominant mode of inhibition, suggesting that parallel inhibitory networks regulate sensory information transmission through the granular layer.

Author contributions: I.D., T.B., P.C., C.A., K.P., and M.H. designed research; I.D., T.B., P.C., C.A., and K.P. performed research; I.D. and T.B. analyzed data; and I.D., T.B., and M.H. wrote the paper.

The authors declare no conflict of interest.

This article is a PNAS Direct Submission.

Freely available online through the PNAS open access option.

[1]I.D. and T.B. contributed equally to this work.

[2]Present address: Centre for Integrative Physiology, School of Biomedical Sciences, University of Edinburgh, Edinburgh EH8 9XD, Scotland.

[3]To whom correspondence may be addressed. Email: ian.duguid@ed.ac.uk or m.hausser@ucl.ac.uk.

[4]Present address: Medical Research Council Laboratory of Molecular Biology, Cambridge CB2 0QH, United Kingdom.

[5]Present address: Department of Bioengineering, South Kensington Campus, Imperial College London, London SW7 2AZ, United Kingdom.

[6]Present address: UCL Institute of Ophthalmology, London EC1V 9EL, United Kingdom.

This article contains supporting information online at www.pnas.org/lookup/suppl/doi:10.1073/pnas.1510249112/-/DCSupplemental.

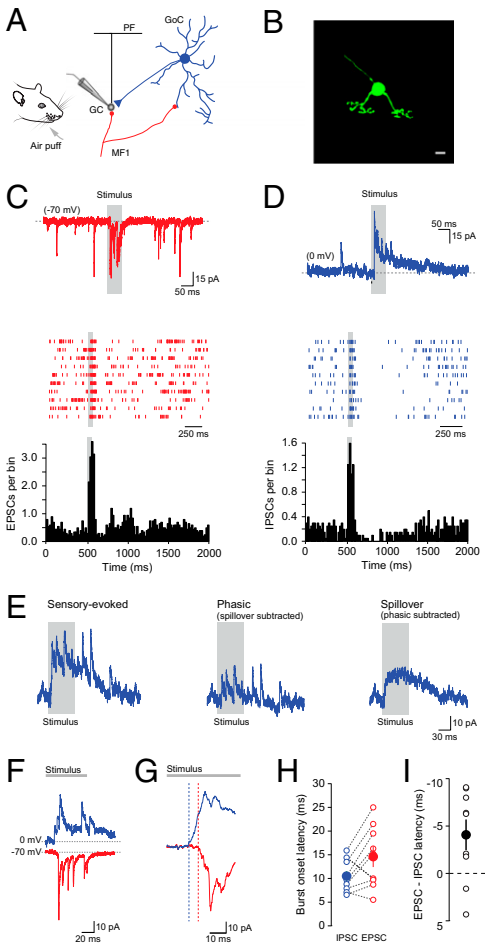

Fig. 1. Sensory-evoked inhibition can precede mossy fiber excitation in cerebellar granule cells. (*A*) Schematic showing the basic circuitry of the granule cell (GC) layer of the cerebellar cortex. GoC, Golgi cell; MF, mossy fiber; PF, parallel fiber. (*B*) Morphological reconstruction of a granule cell obtained by biocytin labeling through the recording electrode and subsequent staining with streptavidin Alexa Fluor 488. (Scale bar: 5 μm.) (*C* and *D*) Voltage-clamp recordings (*Top*), raster plots (*Middle*; 10 trials), and peristimulus time histograms (PSTHs) (*Bottom*; 20 trials; bin size = 20 ms) of spontaneous and stimulus-evoked (gray bar) EPSCs (*C*) and IPSCs (*D*) recorded in a granule cell held at −70 and 0 mV, respectively. (*E*) Example current traces displaying sensory-evoked inhibition (*Left*; V_{hold} = 0 mV) consisting of a burst of phasic IPSCs (*Center*) superimposed on a slow spillover current (*Right*). (*F*) Current traces recorded in a granule cell held at 0 and −70 mV showing the time interval between the onset of sensory-evoked inhibition (blue) and excitation (red). (*G*) Higher-time-resolution example of the relationship between average IPSC and EPSC onset latency (average of 20 consecutive sweeps) in the same granule cell shown in *F*. (*H*) Relationship between IPSC and EPSC onset latencies in individual granule cells (n = 9) with filled symbols representing population average ± SEM. (*I*) Summary plot displaying mean lag between IPSC and EPSC onset times. Negative latency values indicate inhibition preceded excitation (n = 7/9 cells). Filled symbol represents mean ± SEM.

burst of phasic IPSCs was superimposed on a slow, sustained outward current (32.6 ± 4.8 pA; time-to-peak, 22.7 ± 3.5 ms; duration, 308.1 ± 21.4 ms; n = 9; Fig. 1*E*), reflecting GABA spillover (21). Because extrasynaptic δ-subunit–containing $GABA_A$ receptors are insensitive to brief synaptic or spillover GABA transients (26), slow currents are unlikely to reflect changes in the tonic inhibitory conductance (27). In the majority of granule cells, the onset latencies for phasic and spillover events appeared similar, suggesting that both modes of inhibition are driven by the same mossy fiber input pathways. Moreover, the average phasic and spillover peak conductances scaled linearly and were comparable to the excitatory synaptic conductance measured in the same granule cell (Fig. S1). After the short latency excitatory/inhibitory responses in granule cells, we observed a prolonged reduction in spontaneous IPSC rate (duration, 340.0 ± 89.9 ms, n = 6/9 cells), reflecting long-lasting pauses in Golgi cell firing after sensory stimulation (28, 29). Given that Golgi cells fire one or two temporally precise spikes during the onset of sensory stimulation (28, 29)—albeit with variable onset latencies (28, 29)—and that each granule cell receives direct input from at least five to seven Golgi cells (21, 30), our data are consistent with sensory-evoked inhibition being the result of pooled input from multiple Golgi cells.

To investigate whether evoked IPSCs occurred according to the classical excitation–inhibition sequence (6), we examined the relative timing of EPSCs and IPSCs in the same cell during sensory stimulation. Surprisingly, in the majority of granule cells, the mean onset latency of sensory-evoked inhibition was shorter than the latency of direct mossy fiber input evoked by the same sensory stimulus (IPSC latency, 10.5 ± 1.1 ms; EPSC latency, 14.6 ± 2.2 ms; n = 9), contrary to the expectation for a strictly feed-forward pathway (Fig. 1 *F*–*I*). This result suggests that sensory-evoked phasic inhibition of granule cells is mediated by Golgi cells activated by a subset of mossy fibers distinct from those providing direct monosynaptic granule cell excitation (i.e., FFI) or disynaptic feed-forward excitation from granule cells (i.e., feedback inhibition) (15, 31–34). Importantly, this reversed temporal relationship did not depend on the anesthetic regime used (Fig. S2). Given that brief stimulation of the upper lip and perioral surface has been shown to generate precise, short-latency (~7–10 ms) output from Golgi cells (28, 29) and highly variable, longer-latency (~15–25 ms) excitatory input in granule cells (Fig. 1*F*) (23), our data suggest that some Golgi cells receive direct trigeminal input before neighboring granule cells receiving delayed corticopontine input (35, 36).

Properties of Golgi Cell Inhibition During Sustained Sensory-Evoked Mossy Fiber Input. Mossy fiber input to the granule cell layer can occur in short high-frequency bursts (24, 29, 37) or as sustained, time-varying synaptic input (22, 38–40), depending on the nature of the stimulus. To investigate whether stimulus duration affects excitatory and inhibitory sensory-evoked burst dynamics in granule cells in Crus II, we recorded EPSCs (V_{hold} = −70 mV) and IPSCs (V_{hold} = 0 mV) during stimuli of 60-, 200-, and 500-ms duration. Lengthening the stimulus duration linearly increased the number of evoked EPSCs (60 ms: 4.9 ± 0.6; 200 ms: 14.9 ± 2.1; 500 ms: 26.0 ± 4.0 EPSCs; $P < 0.05$, two-way ANOVA with Bonferroni post; n = 9, 8, and 8, respectively) and burst duration (60 ms: 54.8 ± 4.0; 200 ms: 201.3 ± 5.2; 500 ms: 392.5 ± 41.8 ms; $P < 0.01$, two-way ANOVA with Bonferroni post; n = 9, 8, and 8, respectively), initially evoking a burst of high-frequency mossy fiber synaptic input that rapidly decayed to a sustained input frequency of ~50 Hz (Fig. 2 *A*–*D*). Moreover, direct recordings from mossy fiber boutons during sensory stimulation (25) revealed that the patterns of excitatory synaptic input recorded in granule cells directly reflected activity patterns of single presynaptic mossy fiber terminals (Fig. S3 and Table S2). Surprisingly, sensory-evoked phasic and spillover inhibition in granule cells were both unaffected by increasing stimulus duration, with the number and frequency of fast IPSCs and duration of slow IPSCs remaining unchanged (Fig. 2 *E*–*H* and Table S2). Our results indicate that fast phasic inhibition reliably conveys mossy fiber information at the onset of the sensory stimulus, but only weakly conveys rate-based changes in mossy fiber activity during sustained sensory stimulation. In this regard, sensory-evoked Golgi cell inhibition may represent a timing signal during the onset of sensory stimulation.

Classical FFI in Granule Cells In Vivo. We next examined whether classical FFI was detectable at the level of individual events by simultaneously recording sensory-evoked EPSCs and IPSCs at the intermediate holding potential of −40 mV (Fig. 3 *A* and *B*) (6, 41). We observed sensory-evoked events with the characteristic biphasic EPSC–IPSC sequence (mean latency of 2.1 ± 0.1 ms; range 1.9–2.1 ms; Fig. 3*C*) that is the hallmark of FFI (3, 6) in all cells tested (n = 5). However, the rate of occurrence of sensory-

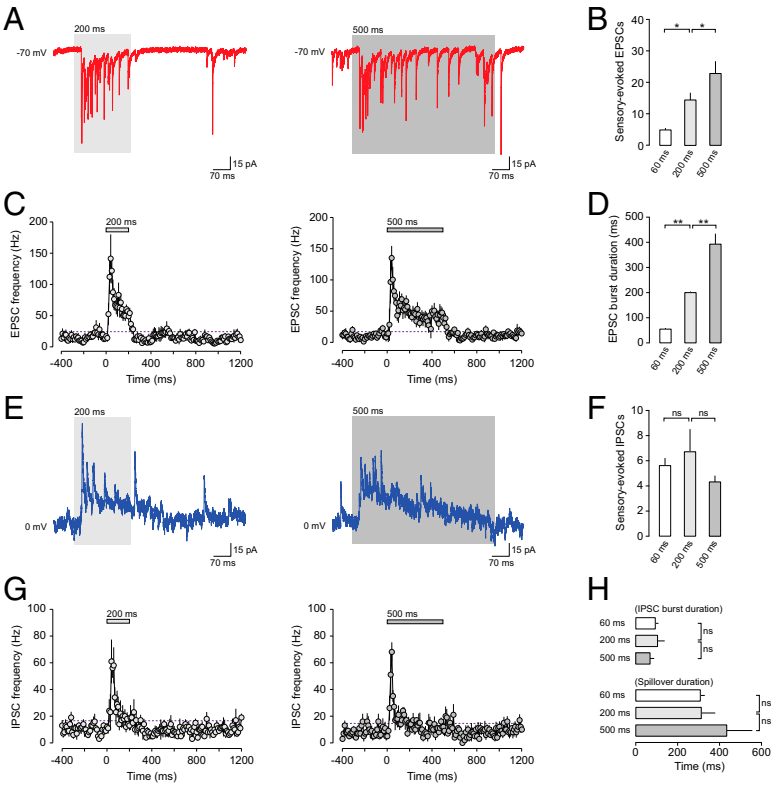

Fig. 2. Sensory-evoked Golgi cell synaptic input in granule cells during sustained sensory stimulation. (*A*) Representative current traces displaying sensory-evoked EPSCs recorded from a granule cell held at −70 mV during prolonged sensory stimulation (200 and 500 ms). (*B*) Average number of EPSCs evoked by 60-, 200-, and 500-ms sensory stimulation (n = 9, 8, and 8, respectively). *P < 0.05. (*C*) PSTHs of EPSC frequency during sustained sensory stimulation (200 and 500 ms; n = 8 and 8). The purple dashed line indicates twofold the SD of the baseline frequency. (*D*) Average sensory-evoked EPSC burst duration evoked by 60-, 200-, and 500-ms sensory stimulation (n = 9, 8, and 8, respectively). **P < 0.01. (*E*) Representative current traces displaying sensory-evoked phasic and spillover inhibition recorded from a granule cell held at 0 mV during 200- and 500-ms sensory stimulation. (*F*) Average number of IPSCs evoked by 60-, 200-, and 500-ms sensory stimulation (n = 9, 5, and 5, respectively). (*G*) PSTHs of IPSC frequency during sustained sensory stimulation (200 and 500 ms; n = 5 and 5). The purple dashed line indicates twofold the SD of the baseline frequency. (*H*) Average sensory-evoked IPSC burst and spillover current duration evoked by 60-, 200-, and 500-ms sensory stimulation (n = 9, 5, and 5, respectively). ns, nonsignificant.

evoked FFI events was low (proportion of FFI events, 18.0 ± 5.1% of total events), comparable to the rate of spontaneous FFI events recorded in granule cells in vivo (23). Moreover, the probability of observing classical FFI was inversely proportional to the variability in IPSC onset latency across each burst, such that a low probability of FFI was associated with larger variability in IPSC timing (Fig. 3*D*). Thus, sensory stimulation can recruit classical feed-forward inhibitory circuits in the granular layer (6, 14), but with relatively low probability, suggesting the majority of sensory-evoked inhibition in granule cells is mediated via the recruitment of parallel inhibitory circuits that are activated via independent mossy fiber pathways (Fig. S4).

Golgi Cell Inhibition Reduces Spike Temporal Fidelity in Granule Cells In Vivo. Previous in vitro findings suggest that feed-forward Golgi cell inhibition acts to reduce the time window for synaptic integration, enforcing granule cell spike precision (6, 28, 29, 42). To assess the impact of Golgi cell inhibition on granule cell spike timing in vivo, we used a dual strategy, combining in vitro dynamic clamp experiments with in vivo intracellular recordings. First, we coinjected simulated trains of mossy fiber input—incorporating frequency-dependent depression (25)—with sensory-evoked inhibition or classical FFI in granule cells in vitro, where the timing and variability of each postsynaptic conductance reflected the EPSC and IPSC onset times measured in vivo (Fig. 4*A*; *Materials and Methods*). We found that inhibition delivered before (sensory-evoked) or 2 ms after (FFI) excitation significantly reduced the temporal precision of early granule cell responses (P < 0.001, two-way ANOVA with Bonferroni post; n = 10) (Fig. 4 *B* and *C*). This result occurs because granule cells require excitatory postsynaptic potential (EPSP) summation during sensory stimulation to generate spiking (24) and Golgi cell inhibition—arriving before or immediately after excitation—suppresses the early response by increasing the number of asynchronous inhibitory events, thus reducing spike probability and increasing jitter. Our in vitro results suggest that Golgi cell inhibition actually reduces the precision of spikes triggered by sensory stimulation. Consistent with this idea, blocking inhibition in vivo with the selective $GABA_A$ receptor antagonist gabazine (SR95531) significantly reduced sensory-evoked first spike jitter in granule cells (Fig. 4 *D*–*G*; n = 7; P < 0.05, two-way ANOVA with Bonferroni post; *SI Materials and Methods*).

Golgi Cell Inhibition Regulates Sensory Response Magnitude and Reproducibility Across Granule Cells. If sensory-evoked Golgi-cell inhibition does not enforce precise spike timing in granule cells, what function does it serve? To address this issue, we examined whether inhibition was important for regulating the magnitude and reproducibility of sensory responses. In this context, magnitude reflects the number of sensory-evoked spikes, whereas reproducibility reflects the average response variability across a population of granule cells. We coinjected simulated trains of mossy fiber input with sensory-evoked inhibition in granule cells in vitro, where the timing and variability of each postsynaptic conductance reflected the EPSC and IPSC onset times measured in vivo (Fig. 5*A*; *Materials and Methods*). We found that sensory-evoked inhibition reduced overall response magnitude by ∼1 spike [−Inh (sensory-evoked) 3.9 ± 0.1 spikes; +Inh (sensory-evoked) 3.1 ± 0.1 spikes; P = 0.01; n = 10] and shortened the duration of the response [−Inh (sensory-evoked) 42.8 ± 0.8 ms; +Inh (sensory-evoked) 38.1 ± 0.7 ms; P = 0.008; n = 10] (Fig. 5 *B*–*D*), while significantly enhancing response reproducibility across granule cells, as indicated by the reduction in variability in evoked response magnitude [FWHM of Gaussian fit to bootstrap histograms: −Inh (sensory-evoked) 0.29; +Inh (sensory-evoked) 0.12; P = 0.003, F test; Fig. 5*C*]. Interburst spike variance (Fig. 5*B*) and average spike burst frequencies (Fig. 5*E*) remained unaffected. Together, our results demonstrate that Golgi-cell inhibition shapes sensory information transmission in the granule cell layer by reducing the temporal fidelity of spikes during the onset of the sensory-evoked response, in favor of enhancing sensory response reproducibility across the granule cell population.

Discussion

We have used voltage-clamp recordings in vivo and dynamic-clamp recordings in vitro to directly assess the impact of inhibitory circuits recruited during sensory information transmission

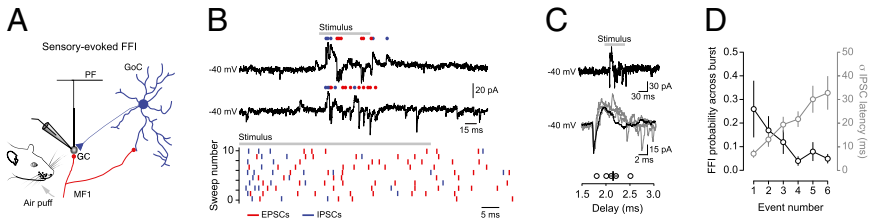

Fig. 3. Low probability of classical FFI in granule cells during sensory stimulation. (*A*) Schematic of the granular layer classical feed-forward inhibitory circuit. GC, granule cell; GoC, Golgi cell; MF, mossy fiber; PF, parallel fiber. (*B*) Voltage-clamp recordings (*Upper*) and raster plot (*Lower*) of sensory-evoked EPSCs (red) and IPSCs (blue) from a granule cell held at −40 mV. (*C*, *Top* and *Middle*) Representative current traces showing sensory-evoked monosynaptic excitation and disynaptic FFI at low (*Top*) and high (*Middle*; average of 20 events overlaid in black) time resolution. (*C*, *Bottom*) Average latency difference between sensory-evoked monosynaptic excitation and disynaptic FFI ($n = 5$). Black bar represents mean value ± SEM. (*D*) Average changes in FFI probability (black) and variability in IPSC onset latency (gray) during sensory-evoked bursts of mossy fiber synaptic input ($n = 5$).

in the granule cell layer of Crus II. We show that Golgi and granule cells within the same local microcircuit receive input via distinct mossy fiber pathways, with excitation often arriving at Golgi cells first, indicating the presence of "parallel" inhibitory networks in the granular layer. In contrast to the prevailing notion that classical FFI enforces precise spike timing in granule cells (6, 14), our findings show that Golgi-cell–mediated inhibition can reduce the temporal precision of early granule cell responses to sensory stimulation, in favor of enhancing sensory response reproducibility across granule cells. Thus, sensory stimuli engage preceding Golgi cell activity, which, by acting through both phasic and spillover inhibition, appears to provide a simple thresholding mechanism to regulate the magnitude and uniformity of sensory responses across granule cells.

Phasic and Spillover Inhibition in Granule Cells In Vivo. Our findings provide, to our knowledge, the first direct characterization of the temporal dynamics of sensory-evoked inhibition in granule cells in Crus II. We demonstrate that brief sensory stimuli evoke short, high-frequency bursts of phasic IPSCs, which are superimposed on a slow sustained outward current, consistent with synchronous direct and spillover input from multiple Golgi cells (6, 21, 26, 28, 29, 43–46). Although fast stimulus-locked inhibition of granule cells has thus far been difficult to detect in vivo (37), our voltage-clamp recordings revealed sensory-evoked phasic and spillover inhibition in all granule cells, consistent with the view that Golgi cell axons strongly influence many hundreds of granule cells across the granular layer (15, 47). Moreover, the prevalence of slow, spillover-mediated IPSCs in granule cells suggests that indirect spillover activation of $GABA_A$ receptors is a major form of Golgi-cell signaling during sensory stimulation (21, 37, 48, 49). Differences in the number of direct and indirect synaptic inputs in each glomerulus will determine the relative contribution of fast and slow IPSCs during sensory activation (21, 30, 49). By recording sensory-evoked excitatory and inhibitory synaptic input in the same cell, we show that sensory-evoked Golgi-cell inhibition scales proportionally with the level of mossy fiber excitatory synaptic input. This finding provides experimental verification of longstanding theories of cerebellar function, which propose that there should be a dynamic component to Golgi-cell inhibition, providing strong inhibition when many mossy fibers are activated and weaker inhibition upon sparse activation of mossy fibers (50, 51). This form of "gain control" regulates the magnitude and saliency of granule cell responses during the onset of sensory stimulation. The fact that we only observed fast-phasic IPSCs during the onset of sensory stimulation is consistent with the view that Golgi cells provide information regarding stimulus onset and that they only weakly follow rate-modulated mossy fiber synaptic input during sustained stimulation (6, 28, 29, 42).

Reversed Excitation–Inhibition Sequence with Sensory Stimulation. The synaptic properties of a classical feed-forward inhibitory circuit are predicted to deliver a rapid inhibitory conductance immediately after sensory-evoked excitation that narrows the window for temporal summation of discrete mossy fiber inputs, thus increasing granule cell spike precision (6, 14). This view forms the basis for many theories of timing in the cerebellar cortex and has been implemented in a variety of cerebellar models (for review, see ref. 7). Our findings challenge this view by demonstrating that the majority of cerebellar granule cells in Crus II receive sensory-evoked Golgi-cell inhibition before the onset of mossy fiber excitation.

Previous studies have shown that peripheral tactile stimulation of the perioral surface and upper lip area in rodents generates coincident activation of direct—via the trigeminal nucleus—and indirect—via a thalamocortico-pontine pathway—input to Crus II of the cerebrocerebellum. Moreover, simultaneous cortical and cerebellar recordings have demonstrated that longer-latency cerebellar inputs reflect cortical output from primary somatosensory cortex (S1) that project to the contralateral cerebellar hemisphere Crus II via the pons (35, 36, 52, 53). Given that recruitment of these two distinct mossy fiber input pathways by the same sensory stimulus can generate precise, short-latency (~7–10 ms) output from Golgi cells (28, 29) and highly variable, longer-latency (~15–25 ms) mossy fiber input to the granule cell layer (Fig. 1) (23, 25, 35), our data are consistent with Golgi cells receiving direct trigeminal input, with nearby granule cells receiving delayed corticopontine input (35, 36). Although the most parsimonious explanation of our data is that Golgi-cell inhibition is mediated via parallel feed-forward inhibitory networks, it is also possible that feedback inhibition plays an important role in regulating sensory-evoked granule cell output. Feedback inhibition—involving disynaptic excitation of Golgi cells via ascending granule cell axons or parallel fibers—has long been suggested on anatomical grounds (15, 47), but experimental evidence to support this observation has been difficult to obtain. Given that granule cell-mediated feedback excitation of Golgi cells provides a powerful feedback circuit to control activity in the granular layer (15, 31–34, 54, 55), it will be important for future studies to identify the extent to which FFI or feedback inhibition contributes to sensory-evoked Golgi cell-mediated inhibition of granule cells in Crus II (Fig. S4).

In addition to revealing the impact of functional parallel inhibitory pathways, our recordings provide direct evidence for the recruitment of classical FFI in granule cells in vivo, where the same mossy fibers exciting a granule cell also provide disynaptic short-latency inhibition to that granule cell via Golgi-cell activation. This feed-forward inhibitory circuit has been suggested on anatomical grounds (15), with in vitro studies demonstrating that disynaptic FFI from Golgi cells can influence the latency and precision of granule-cell responses to mossy fiber stimulation (6, 14, 49). This brief (~5 ms) "time-windowing" effect enhances spike precision by reducing the window for temporal summation of discrete mossy fiber inputs (3, 7). However, our experimental results showing the early onset of sensory-evoked inhibition, the low rate of occurrence of biphasic feed-forward events, and the large trial-to-trial variability in the timing of individual sensory-evoked IPSCs indicate that disynaptic FFI—although functionally engaged in the circuit in vivo—may not be the main determinant of sensory information transmission in granule cells in Crus II. Instead, the early onset and extended temporal profile of sensory-evoked

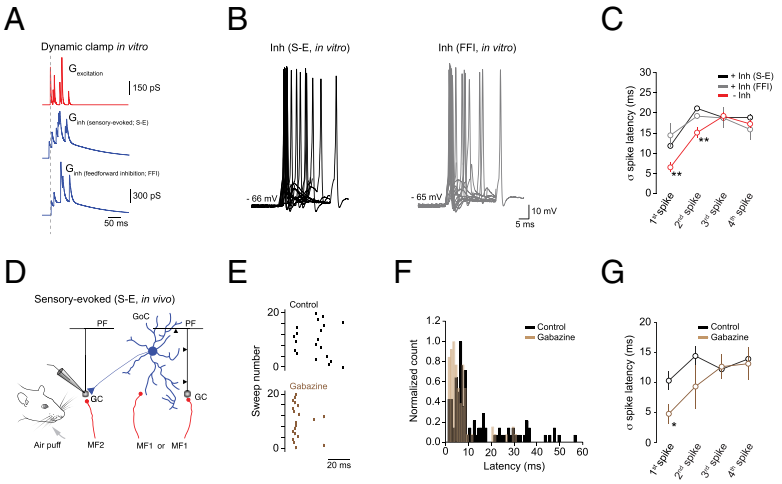

Fig. 4. Golgi cell inhibition reduces the temporal precision of early granule cell responses to sensory stimulation. (*A*) Synaptic conductance waveforms for mossy fiber excitation (*Top*), sensory-evoked inhibition (*Middle*), and classical FFI (*Bottom*). Dashed line denotes onset of the excitatory conductance. (*B*) Example first spike latencies (20 traces overlaid) after coinjection of excitatory ($G_{excitation}$) and inhibitory ($G_{inh\ (sensory\text{-}evoked)}$ or $G_{inh(feed\text{-}forward\ inhibition)}$) conductance waveforms in vitro. Note that intraburst variability, onset timing and peak amplitude of sensory-evoked (S-E) EPSGs and IPSGs faithfully represent our sensory-evoked data recorded in vivo. A steady-state tonic inhibitory conductance (260 pS) was injected to mimic tonic inhibition observed in vivo. (*C*) Average intraburst spike onset latency variability (jitter) in the absence (−Inh, red) and presence of sensory-evoked inhibition [Inh (sensory-evoked); black] or classical FFI [Inh (FFI), gray; $n = 10$]. $^{**}P < 0.01$. (*D*) Schematic representing the recruitment of parallel feed-forward/feedback inhibitory circuits in the granule cell layer during sensory stimulation. GC, granule cell; GoC, Golgi cell; MF, mossy fiber; PF, parallel fiber. (*E* and *F*) Representative raster plots (*E*) and latency histograms (*F*), showing change in sensory-evoked first spike latencies in the absence (black) and presence (brown) of $GABA_A$ receptor blockade (gabazine, 500 μM) in vivo. (*G*) Average variability in sensory-evoked spike onset latency (jitter) in the absence (black) and presence of gabazine (500 μM; brown) ($n = 7$). $^{*}P < 0.05$.

phasic and spillover inhibition suggests that Golgi-cell inhibition provides a simple thresholding mechanism that regulates the amplitude, duration, and reproducibility of sensory responses in granule cells (24, 25, 37). In contrast to sensory modalities that evoke high-frequency mossy fiber input, mossy fibers encoding information about joint angle, head direction, and velocity are tonically active and display relatively slow modulation of their firing rates (38–40). Therefore, it will be of interest to determine the impact of direct and spillover inhibition across a wide range of input modalities and cerebellar regions that display differing rates of mossy fiber activity.

Implications for Sensory Information Processing. Our understanding of the functional role of GABAergic inhibition of granule cells has been constrained by our limited knowledge of the temporal dynamics and varying contributions of phasic and spillover inhibition during sensory stimulation in vivo. The functional characterization of a classical feed-forward inhibitory circuit in the input layer of the cerebellum in vitro (6, 14, 56) led to the assumption that Golgi-cell inhibition plays an important role in regulating both the magnitude and precision of granule cell spike output (6, 14, 18). However, our findings suggest that the primary function of Golgi-cell inhibition in Crus II is not to enforce high temporal fidelity of sensory responses in granule cells, but instead to ensure sensory response uniformity across granule cells. Why might enforcing high cell-to-cell response reproducibility be important for sensory information processing in the granular layer? Given the enormous number of granule cells in the cerebellum (57), the plethora of sensory modalities conveyed by mossy fibers (58), and the high convergence of granule cell axons onto each downstream Purkinje cell (57), it seems necessary that granule cells possess cellular mechanisms that ensure the saliency of important sensory information. The presence of high trial-to-trial and cell-to-cell variability in granule cell sensory responses could introduce a significant level of noise in the mossy fiber–granule cell–parallel fiber pathway, making signal decoding more complex at the level of the Purkinje cell (59). In this regard, we have previously shown that a persistent, tonic GABAergic conductance enhances the ability of granule cells to discriminate sensory-evoked responses from ongoing network activity, where reducing or enhancing tonic inhibition can significantly lower the signal-to-noise ratio for sensory information transmission (23). Our present findings suggest that sensory-evoked phasic and spillover Golgi-cell inhibition provide an additional dynamic regulatory mechanism that scales with the level of mossy fiber excitation controlling the power, duration, and saliency of sensory information as it propagates through the input layer of the cerebellar cortex. Incorporating these findings into existing cerebellar models should provide important insights into how cerebellar microcircuits encode sensory information.

Materials and Methods

In vivo patch-clamp recordings were made from granule cells in Crus II of the cerebellar cortex of 18- to 24-d-old Sprague–Dawley rats anesthetized with a ketamine/xylazine mixture as described (23, 25). Sensory responses were evoked by a brief air puff delivered to the ipsilateral whiskers or perioral surface. All procedures were approved by the local ethical review committee and performed under license from the UK Home Office in accordance with the Animal (Scientific

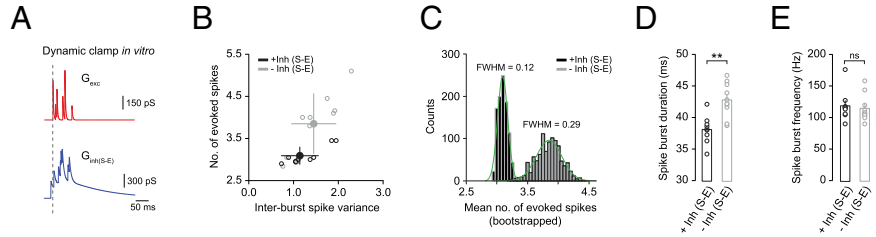

Fig. 5. Parallel FFI enhances sensory response reproducibility across granule cells. (*A*) Simulated synaptic conductance waveforms for mossy fiber excitation (red) and sensory-evoked (S-E) inhibition (blue) were coinjected in granule cells in vitro. Note timing and variability of each postsynaptic conductance reflected the EPSC and IPSC onset times measured in vivo. (*B*) Average number of sensory-evoked spikes as a function of interburst spike variance in the absence [−Inh (sensory-evoked); gray] and presence (black) of sensory-evoked inhibition ($n = 10$). (*C*) Distribution of mean evoked response amplitude in the absence [−Inh (sensory-evoked); gray] and presence (black) of sensory-evoked inhibition estimated by bootstrap analysis (1,000 bootstrap replicates). Green lines are Gaussian fits to each histogram. (*D* and *E*) Average spike burst duration (*D*) and frequency (*E*) with (black) and without (gray) sensory-evoked inhibition ($n = 10$). $^{**}P < 0.01$.

Procedures) Act 1986. Patch-clamp recordings from granule cells in vitro were made at 33–35 °C in cerebellar slices (250 μm thick) prepared with standard techniques (60). For both in vivo and in vitro experiments, patch pipettes (5–7 MΩ) were filled with a potassium methanesulfonate-based internal solution. Data are given as means ± SEM. For full details, see *SI Materials and Methods*.

ACKNOWLEDGMENTS. We thank Ingrid van Welie and Mark Farrant for helpful discussions and for their comments on the manuscript. This work was supported by grants from the Wellcome Trust, European Research Council, Medical Research Council, and the Gatsby Charitable Foundation (to M.H.), and by Wellcome Trust Advanced Training and Research Career Development Fellowships (to I.D.).

1. Wehr M, Zador AM (2003) Balanced inhibition underlies tuning and sharpens spike timing in auditory cortex. *Nature* 426(6965):442–446.
2. Gabernet L, Jadhav SP, Feldman DE, Carandini M, Scanziani M (2005) Somatosensory integration controlled by dynamic thalamocortical feed-forward inhibition. *Neuron* 48(2):315–327.
3. Pouille F, Scanziani M (2001) Enforcement of temporal fidelity in pyramidal cells by somatic feed-forward inhibition. *Science* 293(5532):1159–1163.
4. Atallah BV, Scanziani M (2009) Instantaneous modulation of gamma oscillation frequency by balancing excitation with inhibition. *Neuron* 62(4):566–577.
5. Mittmann W, Koch U, Häusser M (2005) Feed-forward inhibition shapes the spike output of cerebellar Purkinje cells. *J Physiol* 563(Pt 2):369–378.
6. Kanichay RT, Silver RA (2008) Synaptic and cellular properties of the feed-forward inhibitory circuit within the input layer of the cerebellar cortex. *J Neurosci* 28(36):8955–8967.
7. D'Angelo E, De Zeeuw CI (2009) Timing and plasticity in the cerebellum: Focus on the granular layer. *Trends Neurosci* 32(1):30–40.
8. Garrido JA, Ros E, D'Angelo E (2013) Spike timing regulation on the millisecond scale by distributed synaptic plasticity at the cerebellum input stage: A simulation study. *Front Comput Neurosci* 7:64.
9. Medina JF, Mauk MD (2000) Computer simulation of cerebellar information processing. *Nat Neurosci* 3(Suppl):1205–1211.
10. Thach WT (1975) Timing of activity in cerebellar dentate nucleus and cerebral motor cortex during prompt volitional movement. *Brain Res* 88(2):233–241.
11. Spencer RM, Zelaznik HN, Diedrichsen J, Ivry RB (2003) Disrupted timing of discontinuous but not continuous movements by cerebellar lesions. *Science* 300(5624):1437–1439.
12. Walter JT, Alviña K, Womack MD, Chevez C, Khodakhah K (2006) Decreases in the precision of Purkinje cell pacemaking cause cerebellar dysfunction and ataxia. *Nat Neurosci* 9(3):389–397.
13. De Zeeuw CI, Yeo CH (2005) Time and tide in cerebellar memory formation. *Curr Opin Neurobiol* 15(6):667–674.
14. Mapelli J, D'Angelo E (2007) The spatial organization of long-term synaptic plasticity at the input stage of cerebellum. *J Neurosci* 27(6):1285–1296.
15. Eccles JC, Ito M, Szentagothai J (1967) *The Cerebellum as a Neuronal Machine* (Springer, New York).
16. Farrant M, Brickley SG (2003) Properties of GABA(A) receptor-mediated transmission at newly formed Golgi-granule cell synapses in the cerebellum. *Neuropharmacology* 44(2):181–189.
17. Eccles J, Llinas R, Sasaki K (1964) Golgi cell inhibition in the cerebellar cortex. *Nature* 204:1265–1266.
18. Diwakar S, Magistretti J, Goldfarb M, Naldi G, D'Angelo E (2009) Axonal Na^+ channels ensure fast spike activation and back-propagation in cerebellar granule cells. *J Neurophysiol* 101(2):519–532.
19. Maex R, De Schutter E (1998) Synchronization of golgi and granule cell firing in a detailed network model of the cerebellar granule cell layer. *J Neurophysiol* 80(5):2521–2537.
20. Dugué GP, Dumoulin A, Triller A, Dieudonné S (2005) Target-dependent use of co-released inhibitory transmitters at central synapses. *J Neurosci* 25(28):6490–6498.
21. Rossi DJ, Hamann M (1998) Spillover-mediated transmission at inhibitory synapses promoted by high affinity alpha6 subunit GABA(A) receptors and glomerular geometry. *Neuron* 20(4):783–795.
22. Hartmann MJ, Bower JM (2001) Tactile responses in the granule cell layer of cerebellar folium crus IIa of freely behaving rats. *J Neurosci* 21(10):3549–3563.
23. Duguid I, Branco T, London M, Chadderton P, Häusser M (2012) Tonic inhibition enhances fidelity of sensory information transmission in the cerebellar cortex. *J Neurosci* 32(32):11132–11143.
24. Chadderton P, Margrie TW, Häusser M (2004) Integration of quanta in cerebellar granule cells during sensory processing. *Nature* 428(6985):856–860.
25. Rancz EA, et al. (2007) High-fidelity transmission of sensory information by single cerebellar mossy fibre boutons. *Nature* 450(7173):1245–1248.
26. Bright DP, et al. (2011) Profound desensitization by ambient GABA limits activation of δ-containing GABAA receptors during spillover. *J Neurosci* 31(2):753–763.
27. Brickley SG, Cull-Candy SG, Farrant M (1996) Development of a tonic form of synaptic inhibition in rat cerebellar granule cells resulting from persistent activation of GABAA receptors. *J Physiol* 497(Pt 3):753–759.
28. Vos BP, Volny-Luraghi A, De Schutter E (1999) Cerebellar Golgi cells in the rat: Receptive fields and timing of responses to facial stimulation. *Eur J Neurosci* 11(8):2621–2634.
29. Holtzman T, Rajapaksa T, Mostofi A, Edgley SA (2006) Different responses of rat cerebellar Purkinje cells and Golgi cells evoked by widespread convergent sensory inputs. *J Physiol* 574(Pt 2):491–507.
30. Jakab RL, Hámori J (1988) Quantitative morphology and synaptology of cerebellar glomeruli in the rat. *Anat Embryol (Berl)* 179(1):81–88.
31. Dieudonné S (1998) Submillisecond kinetics and low efficacy of parallel fibre-Golgi cell synaptic currents in the rat cerebellum. *J Physiol* 510(Pt 3):845–866.
32. Misra C, Brickley SG, Farrant M, Cull-Candy SG (2000) Identification of subunits contributing to synaptic and extrasynaptic NMDA receptors in Golgi cells of the rat cerebellum. *J Physiol* 524(Pt 1):147–162.
33. Honda T, Yamazaki T, Tanaka S, Nagao S, Nishino T (2011) Stimulus-dependent state transition between synchronized oscillation and randomly repetitive burst in a model cerebellar granular layer. *PLOS Comput Biol* 7(7):e1002087.
34. Buonomano DV, Mauk MD (1994) Neural network model of the cerebellum: Temporal discrimination and the timing of motor responses. *Neural Comput* 6(1):38–55.
35. Morissette J, Bower JM (1996) Contribution of somatosensory cortex to responses in the rat cerebellar granule cell layer following peripheral tactile stimulation. *Exp Brain Res* 109(2):240–250.
36. Diwakar S, Lombardo P, Solinas S, Naldi G, D'Angelo E (2011) Local field potential modeling predicts dense activation in cerebellar granule cells clusters under LTP and LTD control. *PLoS One* 6(7):e21928.
37. Jörntell H, Ekerot CF (2006) Properties of somatosensory synaptic integration in cerebellar granule cells in vivo. *J Neurosci* 26(45):11786–11797.
38. van Kan PL, Gibson AR, Houk JC (1993) Movement-related inputs to intermediate cerebellum of the monkey. *J Neurophysiol* 69(1):74–94.
39. Arenz A, Silver RA, Schaefer AT, Margrie TW (2008) The contribution of single synapses to sensory representation in vivo. *Science* 321(5891):977–980.
40. Barmack NH, Yakhnitsa V (2008) Functions of interneurons in mouse cerebellum. *J Neurosci* 28(5):1140–1152.
41. Häusser M, Clark BA (1997) Tonic synaptic inhibition modulates neuronal output pattern and spatiotemporal synaptic integration. *Neuron* 19(3):665–678.
42. Vos BP, Volny-Luraghi A, Maex R, De Schutter E (2000) Precise spike timing of tactile-evoked cerebellar Golgi cell responses: A reflection of combined mossy fiber and parallel fiber activation? *Prog Brain Res* 124:95–106.
43. Kaneda M, Farrant M, Cull-Candy SG (1995) Whole-cell and single-channel currents activated by GABA and glycine in granule cells of the rat cerebellum. *J Physiol* 485(Pt 2):419–435.
44. Nusser Z, Sieghart W, Stephenson FA, Somogyi P (1996) The alpha 6 subunit of the GABAA receptor is concentrated in both inhibitory and excitatory synapses on cerebellar granule cells. *J Neurosci* 16(1):103–114.
45. Tia S, Wang JF, Kotchabhakdi N, Vicini S (1996) Developmental changes of inhibitory synaptic currents in cerebellar granule neurons: Role of GABA(A) receptor alpha 6 subunit. *J Neurosci* 16(11):3630–3640.
46. Nusser Z, Sieghart W, Somogyi P (1998) Segregation of different GABAA receptors to synaptic and extrasynaptic membranes of cerebellar granule cells. *J Neurosci* 18(5):1693–1703.
47. Palay SL, Chan-Palay V (1974) *Cerebellar Cortex: Cytology and Organization* (Springer, New York), p 348.
48. Hamann M, Rossi DJ, Attwell D (2002) Tonic and spillover inhibition of granule cells control information flow through cerebellar cortex. *Neuron* 33(4):625–633.
49. Crowley JJ, Fioravante D, Regehr WG (2009) Dynamics of fast and slow inhibition from cerebellar golgi cells allow flexible control of synaptic integration. *Neuron* 63(6):843–853.
50. Marr D (1969) A theory of cerebellar cortex. *J Physiol* 202(2):437–470.
51. Albus JS (1971) A theory of cerebellar function. *Math Biosci* 10(1/2):25–61.
52. Wise SP, Jones EG (1977) Cells of origin and terminal distribution of descending projections of the rat somatic sensory cortex. *J Comp Neurol* 175(2):129–157.
53. Brodal P, Bjaalie JG (1997) Salient anatomic features of the cortico-ponto-cerebellar pathway. *Prog Brain Res* 114:227–249.
54. Hull C, Regehr WG (2012) Identification of an inhibitory circuit that regulates cerebellar Golgi cell activity. *Neuron* 73(1):149–158.
55. Cesana E, et al. (2013) Granule cell ascending axon excitatory synapses onto Golgi cells implement a potent feedback circuit in the cerebellar granular layer. *J Neurosci* 33(30):12430–12446.
56. Eccles JC, Llinás R, Sasaki K (1966) The inhibitory interneurones within the cerebellar cortex. *Exp Brain Res* 1(1):1–16.
57. Llinás R, Walton KD, Lang EJ (2004) *The Synaptic Organization of the Brain* (Oxford Univ Press, New York).
58. Arenz A, Bracey EF, Margrie TW (2009) Sensory representations in cerebellar granule cells. *Curr Opin Neurobiol* 19(4):445–451.
59. Steuber V, et al. (2007) Cerebellar LTD and pattern recognition by Purkinje cells. *Neuron* 54(1):121–136.
60. Davie JT, et al. (2006) Dendritic patch-clamp recording. *Nat Protoc* 1(3):1235–1247.